Chromatographic Investigation of CO_2−Polymer Interactions at Near-Critical Conditions

Rebecca R. Edwards, Yingmei Tao, Sihua Xu, Phillip S. Wells, Kwang S. Yun, and Jon F. Parcher*

Chemistry Department, University of Mississippi, University, Mississippi 38677

Received: July 25, 1997; In Final Form: November 24, 1997

A chromatographic method, namely, mass spectrometric tracer pulse chromatography, MSTPC, was used to measure the solubility of carbon dioxide in PMMA, poly(methyl methacrylate), over a wide range of temperatures (−10 to 180 °C) and pressures (<90 atm). In this range of experimental conditions, CO_2 was present as a gas or supercritical fluid and the polymer was either in a glassy or rubbery state (T_g = 100-110 °C). Three lattice theories were evaluated for correlation with the experimental solubility data. The Sanchez−Lacombe, Panayiotou−Vera, and Martire−Boehm models were used to calculate the densities of the pure gas and binary liquid phases from an equation of state and the chemical potential of CO_2 in both the pure gas and polymer mixtures. The solubility of CO_2 in PMMA as a function of temperature and pressure was calculated from these three lattice theory models and compared with the experimental data. Only one temperature-dependent adjustable parameter was used in these calculations to fit the theoretical models to the experimental data.

Introduction

It is well-known that dissolved gases, such as CO_2, can significantly alter the chemical and physical properties of molten (rubbery or liquid) polymers. The physical properties that can be affected include the viscosity, density, diffusivity, and swollen volume. Solvation of a gas, such as CO_2, in a polymer may even induce a glass-to-rubber phase transition as the pressure of CO_2 is increased at a fixed temperature. Increased CO_2 sorption by the polymer results in a reduction of the glass transition temperature presumably because CO_2 facilitates segmental motion in the polymer. In the particular case of carbon dioxide and PMMA, the polymer may even undergo a glass-to-rubber transition as the temperature is *decreased* at a fixed pressure due to the increased sorption of CO_2. This phenomenon has been termed retrograde vitrification.[1] Such effects are most dramatic for supercritical fluids and dense gases at high pressures and/or low temperatures. For these reasons, knowledge of gas solubility and the effects of dissolved gases on the properties of polymers is important for the commercial success of many polymer-processing operations.

Such phenomena are also of crucial interest in chromatographic science especially in the area of SFC, supercritical fluid chromatography, in which the most common stationary liquid phases are very thin films of cross-linked or chemically bonded polymers and carbon dioxide is the most popular SFC mobile phase. Dissolution of the CO_2 from the mobile phase into the polymeric stationary phase can influence both the retention (partition coefficient) and dispersion (diffusion coefficient) of a particular solute. Solution-induced swelling of the polymeric stationary phase diminishes (a) the void volume, (b) the phase ratio of the column, and (c) the retention time of eluted analytes. Thus, a knowledge of gas solubility is also essential to the development of chromatographic theories of retention and resolution.

Fortunately, one of the major advantages of chromatography is the fact that the technique can be used in a somewhat "inverse" manner to investigate exactly those physical properties which are of significant interest in polymer-processing applications and influence the quality of analytical chromatography with solutes at infinite dilution. One chromatographic technique in particular, namely, tracer pulse chromatography,[2,3] is especially suited for the determination of the solubility of gases in liquids and polymers.[4,5] The technique is simple but does require a detector that can distinguish an isotopically labeled tracer in a background of unlabeled (natural) carrier gas. Despite the need for an isotope-specific detector, chromatographic techniques offer some unique advantages over the more classical barometric, volumetric, and gravimetric procedures commonly used to measure sorption of CO_2 in polymers. For example, the experiments are very fast because the polymer is distributed as a relatively thin film (nano- to micrometer thicknesses), so the systems achieve thermodynamic equilibrium rapidly compared to bulk polymers; the systems can be followed through a phase transition as the polymer changes from a glass to a rubber state or vice versa; temperature is easily varied with a GC column oven from subambient to relatively high temperatures (300−400 °C); both subcritical and supercritical mobile phases can be employed with the technique; and the experimental procedure is simple and accurate involving only the measurement of the specific retention volume of a labeled isotopic tracer at a known temperature and pressure.

The earliest sorption measurements of CO_2 in PMMA were carried out in 1981 by Koros, et al.,[6] with a volumetric apparatus. The experimental data measured at three temperatures from 30 to 80 °C up to 20 atm were modeled by a dual-mode model[7−9] in which the sorption is postulated to be composed of two independent contributions. One contribution is a Henry's law type solubility, whereas the second component is a Langmuir type contribution with a nonlinear isotherm that displays a maximum saturation level. Liau and McHugh[10] also used a volumetric apparatus covering a similar temperature range but extended the pressure range up to 250 atm. The classical Flory model was used to interpret this data set in which the interaction parameter was found to be both temperature- and

S1089-5647(97)02430-9 CCC: $15.00
Published on Web 01/22/1998

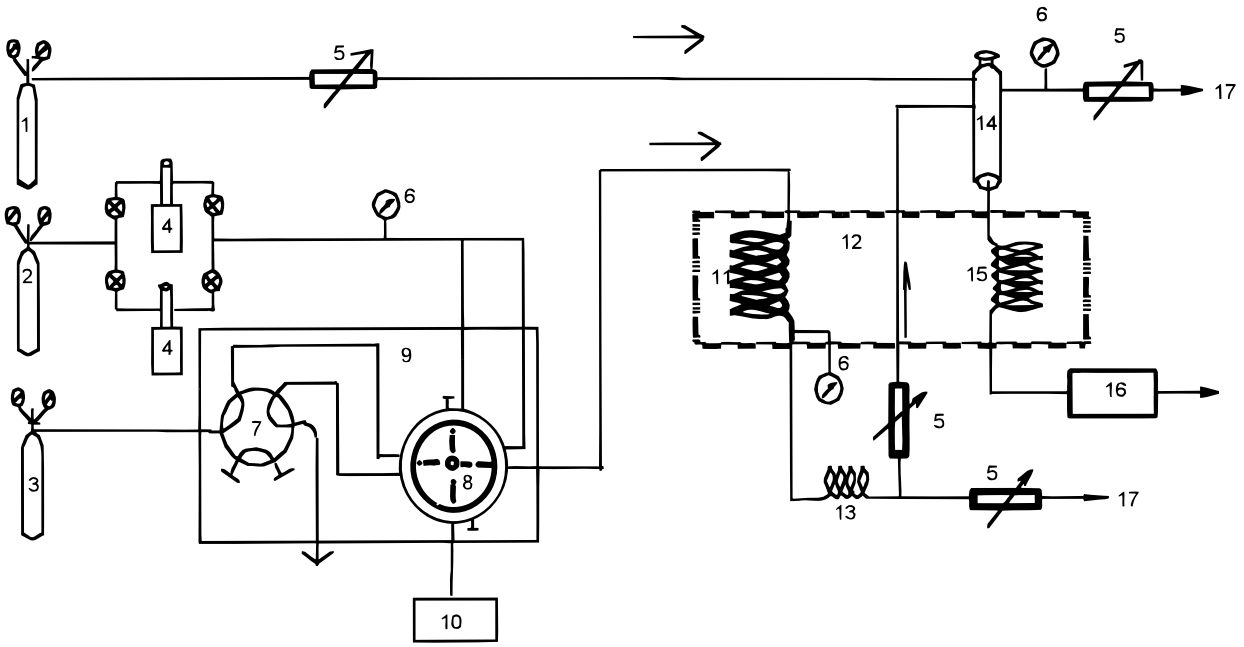

Figure 1. Schematic diagram of the MSTPC instrumentation: (1) carrier gas (He); (2) carrier gas (CO_2); (3) sample gas (Ne and CO_2 isotope); (4) high-pressure pump; (5) flow regulator; (6) pressure sensor; (7) isolation valve; (8) multiposition valve; (9) valve oven; (10) vacuum pump; (11) analytical column; (12) GC oven; (13) capillary restrictor; (14) capillary column injector; (15) uncoated capillary tubing; (16) mass-specific detector; (17) vent.

composition-dependent. Later, Wissinger and Paulaitis[11] used a gravimetric experiment to measure the uptake of CO_2 by PMMA up to 100 atm over the same temperature range. The major experimental uncertainty involved a buoyancy correction that required an accurate estimation of the *volume* of CO_2 absorbed. Extensive theoretical modeling based on the Panayiotou−Vera[12] statistical lattice theory was applied to this data set in a subsequent publication.[13] Most recently, Berens and Huvard[14] developed a novel gravimetric method that avoided in situ mass measurements and thus the uncertain buoyancy correction step. In their original report on the experimental procedure, only a single isotherm at 25 °C for subcritical pressures of CO_2 was reported. Significantly, these authors showed that the temperature dependence of previously reported experimental data could be eliminated by reporting the isotherms in the form of concentration of CO_2 in the polymer phase versus the activity of CO_2.

Three[6,11,14] of these four data sets for the sorption of CO_2 in PMMA agree remarkably well considering the variation in experimental procedures and polymer molecular weights. Thus these three data sets form a combined database which will be used for the validation of the chromatographic data reported herein.

It is the objective of the present studies to establish the validity of the proposed experimental chromatographic method to measure the sorption of gaseous or supercritical CO_2 in either glassy or rubbery polymers over extended temperature and pressure ranges.

Experimental Section

The basic instrument, shown in Figure 1, was an HP 5971 GC/MS system combined with two ISCO syringe pumps (4) with a total capacity of 1000 mL. The injection system was composed of a closed-loop design[15] with a multiposition gas-sampling valve (8). The upper pressure limit of this valve restricted the experimental pressure to 90 atm. The analytical column (11) was a packed column containing PMMA coated on Chromosorb W HP. The inlet and outlet column pressures were monitored via two Setra Model 204 (0−5000 psia) pressure transducers (6). An integral restrictor of 50 μm i.d. capillary tubing (13) was located between the analytical column (11) and the inlet (14) to the GC/MS (16). The length of the restrictor was varied to control the flow rate at different pressures. The flow of CO_2 was split and diluted with helium before introduction into the detector.

The high-pressure sampling valve (8) was a multiposition Valco valve operated by a microelectric actuator under the control of the instrument computer. The four positions of this valve are illustrated in Figure 2. One position of the valve was used to *load* the sample from the reservoir into the sample loop. In the next position, the sample loop was *pressurized* by introduction of CO_2 carrier gas from the system. This pressurization prevented a momentary drop of the system pressure when the loop was introduced into the carrier gas flow path. The third position of the valve allowed for *injection* of the sample from the pressurized loop into the system. In the final position, the high-pressure CO_2 was *evacuated* from the sample loop by a vacuum pump to prevent dilution of the sample reservoir with high-pressure CO_2 when the loop was returned to the *load* position in contact with the closed sample reservoir.

Neon served as a dead time marker and the isotopic CO_2 acted as a tracer to measure the total amount of CO_2 in both phases. The carrier gas was natural CO_2 . The mass-selective detector was set to monitor $m/z = 20$ (neon) and $m/z = 47$ ($^{13}C^{18}O^{16}O$) so these species could be detected in a high background of natural CO_2. The carrier gas volume flow rate was measured at ambient conditions. The molar flow rate, F_m, was calculated from the ideal gas law using the measured outlet volume flow rate at ambient temperature and pressure. The total number of moles of CO_2 in the system, n_{CO_2}, was determined from the molar flow rate and the retention time of the isotopic CO_2, t_R*, from the relation $n_{CO_2} = t_R{*}F_m$. The amount of CO_2 in the mobile phase, $n^m_{CO_2}$, was determined from the retention time of the neon peak $n^m_{CO_2} = t_{R,Ne}F_m$. The

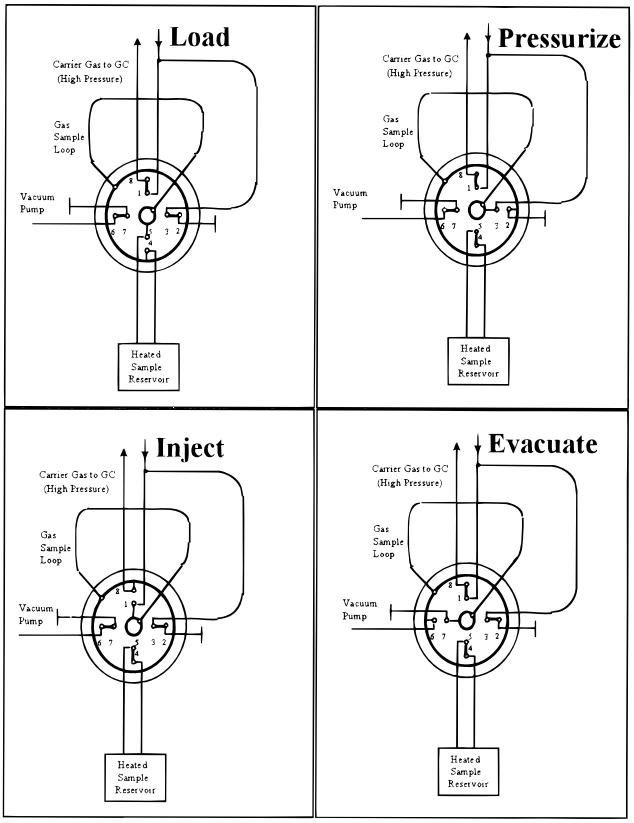

Figure 2. Multiposition gas-sampling valve.

amount of CO_2 dissolved in, or adsorbed on, 1 g of polymer, $n^{P}_{CO_2}$, was determined by difference as shown in eq 1

$$n^{P}_{CO_2} = \frac{n_{CO_2} - n^{m}_{CO_2}}{w_s} \tag{1}$$

where w_s is the weight of the polymer.

The data reported herein were converted from moles of CO_2 per gram of polymer, $n^{P}_{CO_2}$, to the more commonly used engineering units of [mL (STP)/g polymer] for comparison with previously published literature data.

The thickness of the polymer films used in this study was crucial. The solubility of CO_2 in very thin films of the polymer was significantly lower than the solubility in bulk polymer films. To achieve the necessary thicknesses, Chromosorb W HP which has a surface area of approximately 1 m^2/g was used as the solid support. A high percent coating of the polymer on this support led to films with thicknesses that varied between approximately 0.1 and 0.2 μm. Other solid supports, such as Chromosorb P with a surface area of 5 m^2/g, led to films of only 0.02-0.04-μm thicknesses at the same percent coating. Only solubility data obtained with films greater than 0.1 mm were comparable to data from bulk polymers.

Results and Discussion

The proposed chromatographic technique differs in two important ways from the previously published methods for the measurement of the sorption of CO_2 in polymers. Firstly with chromatographic methods, it is relatively easy to measure the Henry constant for other components as a function of the pressure of CO_2 or as a function of the volume fraction of CO_2 sorbed in the polymer. Classical methods, however, cannot distinguish between the solubilities of more than one component without a complete analysis of both phases.

TABLE 1: Experimentally Measured Sorption of CO_2 in PMMA at Various Temperatures and Pressures

Amount of CO_2 Sorbed (mL(STP)/g polymer)						
Temperature (^{0}C)	Pressure (atm)					
	15	30	45	60	75	90
-10	46.1	Two-Phase Region for CO_2			*a*	
0	40.2	78.4				
10	29.4	67.7				
20	25.0	55.8	74.9			
30	22.0	42.1	60.7	88.6	115.3	
40	19.2	36.6	48.9	72.4	90.4	129.7
50	15.6	28.2	40.6	59.3	73.7	99.1
60	12.6	23.3	34.4	50.4	60.3	74.7
70		19.9	29.2	43.5		59.3
80	8.6	16.9	25.3	36.6	47.0	55.7
90		14.9		32.5		50.0
100	6.7	13.4	20.2	28.3	33.8	46.0
110		11.9		24.9		36.4
120	5.4	10.9	17.0	22.9	28.1	37.2
140	4.5	9.4	14.1	19.4	22.7	30.5
160	4.1	8.1	12.2	16.5	19.5	21.3
180	3.4	7.2	10.8	13.8	17.3	17.4

[a] At pressures of 75 and 90 atm, a small change in temperature at temperatures less than 30 °C causes a large change in the solubility of CO_2 in PMMA. In a chromatographic experiment, this leads to a long retention time of the isotopic CO_2; thus, experiments were not carried out at these lower temperatures.

Secondly, it is possible to carry out the chromatographic experiments in either an isothermal or isobaric mode. Most gravimetric and volumetric methods are designed for isothermal operation because it is much easier to alter the pressure than the temperature of most experimental sorption apparatus. On the other hand, it is relatively easy to change the temperature of a chromatographic oven. For this reason, the sorption experiments were carried out in an isobaric mode at equal temperature increments; thus, isotherms could be constructed from the isobaric data. The experimental results are given in Table 1 as a function of temperature and pressure.

Figure 3 shows the data from Table 1 plotted as isobars. Figure 3A shows data for 30, 60, and 90 atm, while Figure 3B has the 15, 45, and 75 atm isobars. The chromatographic data from the present study are shown as open circles. Data from the three literature data sets[6,11,14] are also plotted in the figure. These data sets were obtained under isothermal conditions at varying pressures. For comparison with the chromatographic data, the literature data were interpolated to the experimental pressures used in this study.

To test the thermodynamic consistency of the data set, the activity of CO_2 in the polymeric phase was calculated from eq 2.[16,17] The activity of CO_2, A_{CO_2}, is defined as the ratio of the fugacity of CO_2 in any state to the fugacity of CO_2 in a standard state.

$$A_{CO_2} = \frac{P_{CO_2}\gamma_{CO_2}(T,P)}{P_{CO_2}{}^{sat}\gamma_{CO_2}(T,P^{sat}) \exp\left\{\frac{\bar{v}_{CO_2}}{RT}(P - P^{sat})\right\}} \tag{2}$$

The gas-phase fugacity of pure CO_2 was determined from the Peng−Robinson equation of state.[18] At equilibrium, the fugacity of CO_2 in the gas phase must equal the fugacity of CO_2 in the

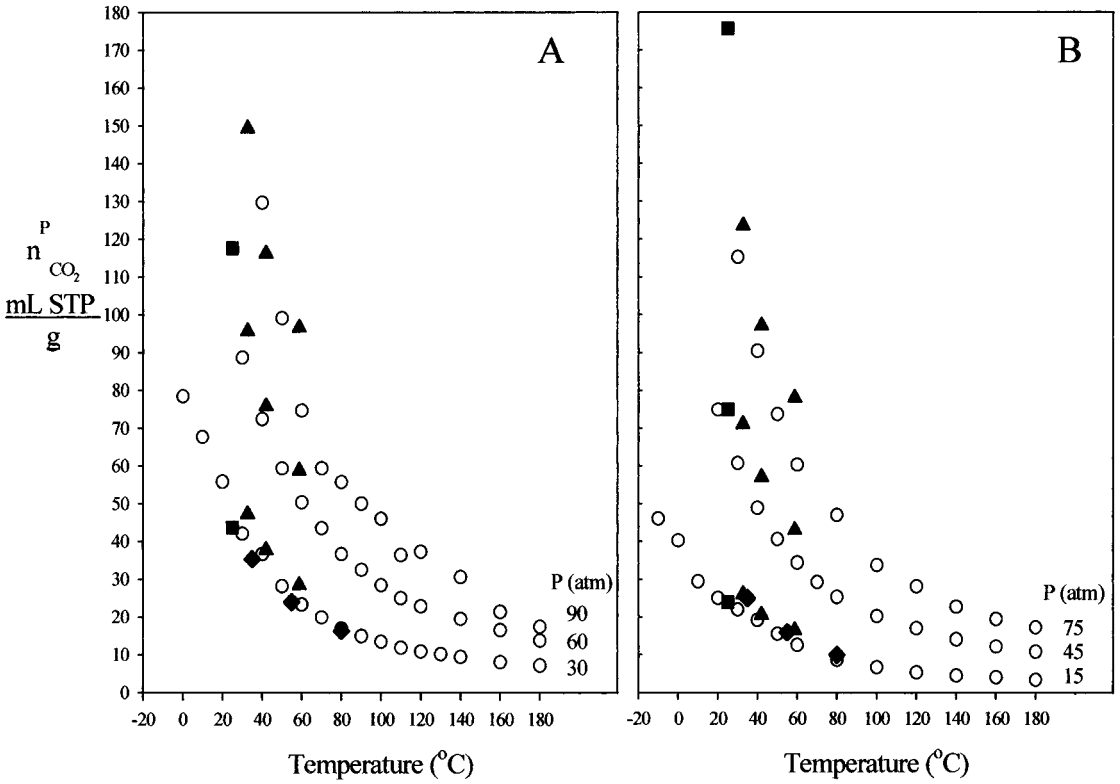

Figure 3. Comparison of solubility data with previously published results: (○) this work (tracer pulse chromatography), (■) Berens and Huvard[14] (gravimetric), (▲) Wissinger and Paulaitis[11] (gravimetric) (◆) Koros, Smith and Stannett[6] (volumetric).

polymeric phase. The standard state of CO_2 in the polymer phase was taken to be pure liquid CO_2 at the saturated vapor pressure. At pressures above the critical point, a hypothetical saturated vapor pressure was calculated by extrapolation. In eq 2, the term $\gamma_{CO_2}(T,P)$ is the fugacity coefficient of CO_2 and $\bar{v}_{CO_2}$ represents the partial molar volume of liquid CO_2 (46.2 mL/mol).[19]

The volume fraction, Φ_{CO_2}, was calculated from the primary data, $n^P_{CO_2}$, by the following transformation:

$$\Phi_{CO_2} = \frac{n^P_{CO_2}\bar{v}_{CO_2}}{n^P_{CO_2}\bar{v}_{CO_2} + \frac{1}{\rho_{Poly}}} \quad (3)$$

where ρ_{Poly} represents the density of PMMA. The density of the polymer at various temperatures and pressures was determined from the data of Olabisi and Simha.[20]

Part A of Figure 4 shows the three previously mentioned literature data sets[6,11,14] plotted in the form of volume fraction versus the activity of CO_2 in the condensed phase. This type of data presentation was used by Berens[14] to eliminate the temperature dependence commonly observed for pressure-based isotherms. The line shown in Figure 4 was calculated from the Flory−Huggins equation,[21] which is the most commonly used basic model for the interpretation of solubility data for polymers. This equation relates the activity of CO_2 in the polymer to the volume fraction of polymer, Φ_{Poly}, in the CO_2−polymer mixture:

$$\ln A_{CO_2} = \ln(1 - \Phi_{Poly}) + \left(1 - \frac{r_{CO_2}}{r_{Poly}}\right)\Phi_{Poly} + \chi\Phi_{Poly}^2 \quad (4)$$

where r_{CO_2} and r_{Poly} represent the size of a CO_2 and polymer molecule, respectively. The interaction parameter, χ, is a measure of the energy for CO_2−polymer interactions. A linear regression of eq 4 with the experimental data from Table 1 was

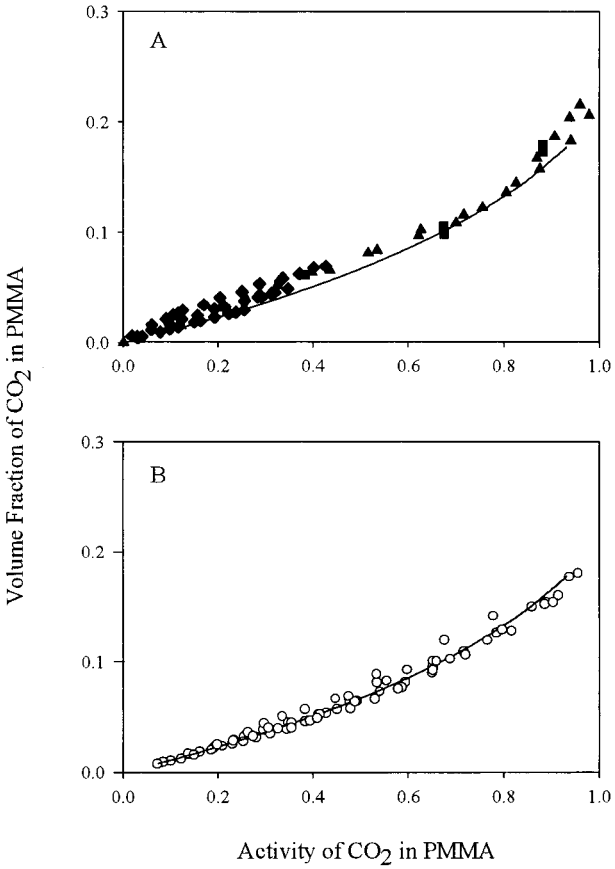

Figure 4. Volume fraction vs activity plots. (A) Literature data: (■) Berens and Huvard,[14] (▲) Wissinger and Paulaitis,[11] (◆) Koros, Smith, and Stannett.[6] (B) (○) Data from Table 1.

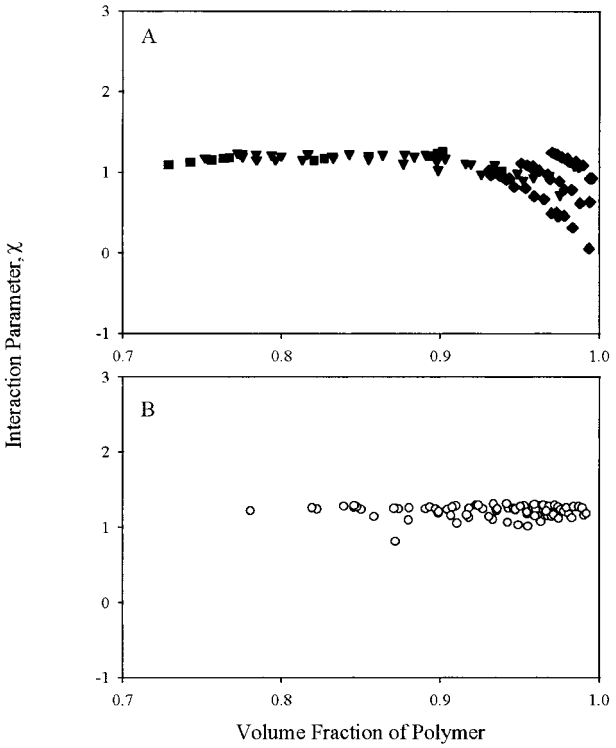

Figure 5. Flory−Huggins interaction parameters. (A) Literature Data: (■) Berens and Huvard,[14] (▼) Wissinger and Paulaitis,[11] (◆) Koros, Smith, and Stannett.[6] (B) (○) Data from Table 1.

performed with χ as the single adjustable parameter and the ratio r_{CO_2}/r_{poly} assumed to approach zero. The best fit line ($\chi = 1.235$) is shown in both parts A and B of Figures 4. Thus, the chromatographic solubility data given in Table 1 are in excellent agreement with previous data obtained over more limited ranges of temperature and pressure.

Figure 5 is a plot of χ versus Φ_{Poly} for the same data sets shown in Figure 4. In this case, the value of χ which produced exact agreement between experimental and calculated values of the activity in eq 4 was determined for each data point. At high volume fractions of polymer, the literature data show some grouping into isotherm sets, and there is more scatter of the χ values at low concentrations of CO_2. Such composition and temperature dependence of χ have been previously reported.[10,22,23] For these reasons, the Flory−Huggins equation is not an adequate model, especially for very dilute solutions of CO_2 in the polymer. Figure 5B shows the same comparison for the data from Table 1, and there is less scatter and no obvious grouping into isotherm sets. This comparison, however, points out some of the difficulties of displaying multidimensional data in a two-dimensional form. The most probable reason for the linearity shown in Figure 5B is that the data for high volume fractions of polymer in the present study were obtained at high temperatures, whereas the same range of data in Figure 5A were obtained at low pressure and low temperature, where the Flory−Huggins equation is less reliable. Thus a simple, two-dimensional plot with composition as the independent variable obscures the roles of both temperature and pressure in the determination of composition.

The experimental data reported herein over large temperature and pressure ranges agree well with the literature sorption data. This more extensive set of chromatographic data was used to evaluate three theoretical models that describe CO_2 sorption by polymers.

Theoretical (Lattice Fluid Models)

Several lattice fluid models have been developed to describe the sorption of gases by polymers. Details of the various versions differ; however, there are some common features involving concentration scales and reduced (dimensionless) pressure, temperature, density, and size parameter expressions. All of the models assume that the gases and polymers are composed of units (mers) which each occupy one site on a lattice that may contain empty lattice sites. Molecular species are treated as *r*-mers where *r* is the number of mers per molecule. The following definitions are common to many of the lattice theories. (Quantities denoted with a tilde are dimensionless (reduced) quantities; those with a superscript * are characteristic quantities; those with a subscript refer to a particular component; and those without a subscript refer to the system.)

Definitions. *Pure Component. Reduced Density.* $\tilde{\rho}_i \equiv \rho_i/\rho_i^*$ where ρ_i^* is the characteristic, hard-core density of component *i* in an incompressible state at 0 K. The reduced density is also a measure of the fraction of lattice sites occupied, i.e., $\tilde{\rho}_i = r_i N_i/(N_0 + r_i N_i)$ where N_0 is the number of vacant lattice sites; and N_i is the number of *r*-mers of component *i*. Thus, $\tilde{\rho}_i$ can be considered as a concentration scale based on the total number of lattice sites even though only one component is present in the system.

Reduced Temperature. $\tilde{T}_i \equiv T_i/T_i^*$ where T_i^* is the characteristic temperature of component *i* and $T_i^* \equiv \epsilon_{ii}^*/R$ where *R* is the gas constant, $R = N_A k$ (Avogadro's number times the Boltzmann constant) and ϵ_{ii}^* is the molar interaction energy for two mer units of component *i*. T_i^* will differ for each component; it will vary with composition for a mixture; and it may even vary with temperature if ϵ_{ii}^* is temperature-dependent.

Reduced Pressure. $\tilde{P}_i \equiv P_i/P_i^*$ where P_i^* is the characteristic pressure or cohesive energy density, i.e., $P_i^* = \epsilon_{ii}^*/\nu_i^*$ where ν_i^* is the characteristic, hard-core volume per mole of mers of component *i* in an incompressible state at 0 K.

Size Parameter. $r_i = m_i P_i^*/\rho_i^* R T_i^* = m_i/\rho_i^* \nu_i^*$, where m_i is the molar mass of component *i* and the product $\rho_i^* \nu_i^*$ represents the molar mass of a mer of component *i*.

The characteristic quantities are related by the expression $RT_i^* = P_i^* \nu_i^*$.

Binary Mixture of a Gas or Fluid in a Polymer. Reduced Density of the Mixture. $\tilde{\rho} = \sum r_i N_i/(N_0 + \sum r_i N_i) = \sum r_i N_i/M$ where *M* is the total number of lattice sites in the system. The reduced density defines a concentration scale involving both empty and occupied lattice sites. The reduced density is simply the fraction of lattice sites that are occupied.

Hard-Core Volume Fraction of Component 1. $\phi_1 = r_1 N_1 \nu^*/\nu^* \sum r_i N_i$ where ν^* is the mer volume (lattice site volume) for the system, which may be treated as a fixed quantity or allowed to vary with composition.

Size Parameter for the Mixture. $1/r = \phi_1/r_1 + \phi_2/r_2 = 1/(x_1 r_1 + x_2 r_2) = 1/\tilde{\rho}\{\tilde{\rho}_1/r_1 + \tilde{\rho}_2/r_2\}$ where x_i is the mole fraction of component *i* in the mixture.

Sanchez−Lacombe (S−L) Equation of State. Sanchez and Lacombe[24−26] have developed several versions of a model that extends the basic Flory−Huggins treatment to mixtures of compressible fluids and polymers. Solubility calculations are performed by finding the composition of the condensed CO_2−polymer mixture that gives a chemical potential for CO_2 in the condensed phase that is equal to the chemical potential of pure CO_2 in the gas or fluid phase at a given temperature and pressure. Calculation of the chemical potential requires the application of an equation of state to determine the reduced density, $\tilde{\rho}$, of the two phases in equilibrium.

CO_2 in the Fluid (Gas) Phase. The chemical potential of pure CO_2 (component 1) in the gas or fluid phase, $\mu_1^{\text{fluid}}(T,P)$, is given by[26]

$$\frac{\mu_1^{\text{fluid}}(T,P)}{RT} = r_1\left[\frac{1-\tilde{\rho}_1}{\tilde{\rho}_1}\ln(1-\tilde{\rho}_1)\right] + \ln\tilde{\rho}_1 - \frac{r_1\tilde{\rho}_1}{\tilde{T}_1} + \frac{r_1\tilde{P}_1}{\tilde{T}_1\tilde{\rho}_1} \quad (5)$$

Commonly, the values of T^*, P^*, and ρ^* are determined from pure component data, such as vapor pressure. The value of r_1 can be calculated from characteristic parameters along with the molar mass using the equation for the size parameter given in the common definitions above. In most treatments, the reduced density, $\tilde{\rho}$, is calculated from an empirical or theoretical equation of state. The S−L lattice fluid EOS for component i is[26]

$$\frac{\tilde{P}_i}{\tilde{T}_i} = -\ln(1-\tilde{\rho}_i) - \tilde{\rho}_i\left(1-\frac{1}{r_i}\right) - \frac{\tilde{\rho}_i^{\,2}}{\tilde{T}_i} \quad (6)$$

CO_2 in the Polymer. The chemical potential of the gas dissolved in the polymer can be obtained from the expression[25]

$$\frac{\mu_1^{\text{polymer}}}{RT}(T,P,\phi_1) = r_1\left[\frac{1-\tilde{\rho}}{\tilde{\rho}}\ln(1-\tilde{\rho})\right] + \ln\tilde{\rho} - \frac{r_1\tilde{\rho}}{\tilde{T}_1} + \frac{r_1\tilde{P}_1}{\tilde{T}_1\tilde{\rho}} + r_1\tilde{\rho}\chi_{12}\phi_2^{\,2} + \phi_2\left(1-\frac{r_1}{r_2}\right) + \ln\phi_1 \quad (7)$$

The EOS for the mixture is the same as that for a pure component (eq 6) but with r, $\tilde{\rho}$, $\tilde{P}$, and $\tilde{T}$ calculated as average values for the mixture. The size parameter r is calculated from the common mixing rule. The reduced density is obtained from the EOS. The details for the calculation of P^* , T^*, and ν^* vary from one treatment to another. In the present work, however, the approach suggested by Sanchez−Lacombe in a 1978 paper[25] was followed. That is, the composition-dependent lattice site volume, ν^*, was calculated from the relation $\upsilon^* = \phi_1\nu_1^* + \phi_2\nu_2^*$. The characteristic pressure for the binary mixture was calculated from the relation

$$P^* = P_1^*\phi_1 + P_2^*\phi_2 - \phi_1\phi_2\{P_1^* + P_2^* - 2\zeta\sqrt{P_1^*P_2^*}\} \quad (8)$$

where ζ is the only mixture property and was treated as an adjustable parameter. The characteristic temperature was obtained from the calculated values of P^* and ν^*.

In the calculation of $\mu_1^{\text{polymer}}(T,P,\phi_1)$, a value of ϕ_1 is assumed; the characteristic parameters for the mixture at that composition are calculated; $\tilde{\rho}$ is obtained from the EOS, and the chemical potential is calculated from eq 7 with the interaction parameter obtained from the relation.

$$\chi_{12} = \frac{\nu^*}{RT}\{P_1^* + P_2^* - 2\zeta\sqrt{P_1^*P_2^*}\}$$

Then $\Delta\mu_1 = \mu_1^{\text{polymer}} - \mu_1^{\text{fluid}}$ is evaluated and the composition adjusted until $\Delta\mu_1 \rightarrow 0$. The weight fraction, w_1 , of CO_2 in the polymer was obtained from the hard-core volume fraction by the relation

$$w_1 = \frac{\rho_1^*\nu_1^*\phi_1}{\rho_1^*\nu_1^*\phi_1 + \rho_2^*\nu_2^*\phi_2}$$

and the amount of CO_2 absorbed in the polymer, S, in mL-(STP)/g was obtained from the relation

$$S = \frac{22\,415}{m_1}\frac{w_1}{w_2}$$

To determine the best single value for the mixture parameter, ζ, the number that gave exact agreement between experimental and theoretical sorption values was calculated for each experimental data point using pure component values for T^*, P^*, and ρ^* given by Condo et al.[1] Linear regression of the mixture parameter data with respect to temperature yielded an expression $\zeta = 1.05 + 3.3 \times 10^{-4}t$ (°C) with a correlation coefficient of 0.88.

Panayiotou−Vera (P−V) Equation of State. In the Sanchez−Lacombe[24−26] model, the volume of a lattice site was allowed to vary with composition. This inconvenient concept was eliminated in the treatment of Panayiotou and Vera[12] by simply fixing the value of ν^* to a constant for all components. In this sense, the P−V model is considerably simplified compared to the S−L model; however, Panayiotou−Vera also introduced the concept of nonrandom distribution of the components and voids on the lattice sites. A finite coordination number, z, was also retained and assigned a value of 10.

Wissinger and Paulaitis[13] recently used the P−V model to interpret a set of gas solubility data, and the calculation used in the present work follows the approach developed in that study. The calculation algorithm was very similar to that used with the S−L model discussed previously.

CO_2 in the Fluid (Gas) Phase. The P−V equation for the chemical potential of pure CO_2 in the gas (fluid) phase is[12]

$$-\frac{\mu_1^{\text{fluid}}}{RT}(T,P) = \ln\left(\frac{r_1}{\tilde{\rho}_1}\right) + \frac{(q_1 - r_1\tilde{P}_1)}{\tilde{T}_1} + \frac{zq_1}{2}\ln\left\{\frac{\frac{1}{\tilde{\rho}_1} + \frac{q_1}{r_1} - 1}{\Gamma_{11}/\tilde{\rho}_1}\right\} \quad (9)$$

where q_1 is a surface area factor introduced to allow for the loss of nearest neighbor interactions between chemically bonded mers. This factor was calculated from the relation $zq_1 = (z-2)r_1 + 2$. Γ_{11} is a factor introduced to allow for the nonrandom distribution of mers of component 1 on the lattice. The details for the calculation of this factor are given in the original publication.[12]

The reduced density, $\tilde{\rho}_1$, is required to solve eq 9 and can be calculated from the P−V equation of state as given by the expression[12]

$$\frac{\tilde{P}_1}{\tilde{T}_1} = \ln\left\{\frac{1}{1-\tilde{\rho}_1}\right\} + \frac{z}{2}\ln\left\{\frac{\frac{1}{\tilde{\rho}_1} + \frac{q_1}{r_1} - 1}{\Gamma_{00}/\tilde{\rho}_1}\right\} \quad (10)$$

where Γ_{00} is the nonrandom factor for the distribution of empty sites on the lattice.

CO_2 in the Polymer. Likewise the chemical potential of CO_2 dissolved in the polymer at T and P is given by the expression[27]

$$-\frac{\mu_1^{\text{polymer}}}{RT}(T,P,\phi_1) = r_1 \ln(1-\theta) - \ln\left(\frac{\eta_1\theta}{q_1}\right) - \frac{zq_1}{2}\ln \dot{\Gamma}_{11} + q_1\theta\left(\frac{1}{\tilde{T}_1}+\frac{1}{\tilde{T}}\right) + \frac{(r_1-q_1)\theta^2}{\tilde{T}} \quad (11)$$

where the new terms θ and η_1 represent concentration scales based on q_1 rather than r_1 including and excluding empty sites, respectively. Similarly, $\dot{\Gamma}_{11}$ is a factor for the nonrandom distribution of mers of component 1 on the lattice. Details for the calculation of these parameters are given in Wissinger's dissertation.[27]

The equation of state for the mixture is slightly different than that for the pure components.[12]

$$\frac{\tilde{P}}{\tilde{T}} = \ln\left\{\frac{1}{1-\tilde{\rho}}\right\} + \frac{z}{2}\ln\left(1+\frac{\tilde{\rho}q}{r}-\tilde{\rho}\right) - \frac{\theta^2}{\tilde{T}} \quad (12)$$

The algorithm for calculating the condensed-phase composition that will produce equal chemical potentials for CO_2 in both phases is the same as described for the Sanchez−Lacombe treatment.

The r value for the mixture was calculated from the mixing rule based on mole fraction, and the interaction energy, ϵ^*, was determined from the relation

$$\epsilon^* = \eta_1\epsilon_{11} + \eta_2\epsilon_{22} - \eta_1\eta_2\dot{\Gamma}_{12}(\epsilon_{11}+\epsilon_{22}-2\zeta\sqrt{\epsilon_{11}\epsilon_{22}}) \quad (13)$$

Again, ζ was treated as an adjustable parameter. P^* was calculated from ϵ^* and v^*, which was fixed at a value of 9.75 mL/mol.[13] T^* was calculated from ϵ^*/R. The linear regression results for all of the data in Table 1 resulted in the equation $\zeta = 0.97 - 4.0 \times 10^{-4}t$ (°C) with a correlation coefficient of 0.95.

Martire and Boehm (M−B) Equation of State. Martire and Boehm[28] proposed an isotherm equation that is a natural extension of the Flory−Huggins and Sanchez−Lacombe theories. The major improvement over the previous theories was the fundamental application of the concept of Helmholtz free energy, A, instead of the Gibbs free energy used by previous investigators. Instead of constant pressure, this model was developed in terms of constant volume (constant number of lattice sites, M.) This approach allowed the authors to combine the chemical potential and equation-of-state equilibrium requirements to produce a single isotherm equation that relates the composition of the condensed phase directly to the temperature and density of the pure gas phase. This equation was derived by simultaneously imposing two conditions for equilibrium of CO_2 between the stationary (polymer) and mobile (fluid) phases, namely, the chemical potential in terms of the Helmholtz free energy

$$\frac{\mu_i}{RT} = \frac{\partial}{\partial N_i}\left\{\frac{A}{RT}\right\}_{T,M,N_j}$$

and the dimensionless pressure-to-temperature ratio,

$$\frac{\tilde{P}}{\tilde{T}} = \frac{Pv^*}{RT} = -\frac{\partial}{\partial M}\left\{\frac{A}{RT}\right\}_{T,N_i,N_j}$$

The chemical potential equivalence requirement can be expressed by the relation

$$\frac{zr_1}{RT}(\theta_1\epsilon_{11}+\theta_2\epsilon_{12}) + \ln\left(\frac{\theta_1}{r_1}\right) - r_1\ln(1-\theta_1-\theta_2) = \frac{zr_1}{RT}\tilde{\rho}_1\epsilon_{11} + \ln\left(\frac{\tilde{\rho}_1}{r_1}\right) - r_1\ln(1-\tilde{\rho}_1) \quad (14)$$

where $\theta_1 = r_1N_1v^*/Mv^*$. The expression $1-\theta_1-\theta_2$ represents the fraction of empty sites (free volume) in the polymer. If $N_0 \rightarrow 0$ in the polymer, then $\theta_1 \rightarrow \phi_1$.

Likewise, the equilibrium requirement for $\tilde{P}/\tilde{T}$ can be expressed as

$$-\ln(1-\theta_1-\theta_2) - \theta_1\left(1-\frac{1}{r_1}\right) - \theta_2\left(1-\frac{1}{r_2}\right) + \frac{z}{2RT}(\theta_1^2\epsilon_{11}+2\theta_1\theta_2\epsilon_{12}+\theta_2^2\epsilon_{22}) = -\ln(1-\tilde{\rho}_1) - \tilde{\rho}_1\left(1-\frac{1}{r_1}\right) + \frac{z}{2RT}\tilde{\rho}_1^2\epsilon_{11} \quad (15)$$

Multiplying this equation by r_1, taking the difference between these two equations (eq 15 − eq 14), and eliminating common terms gives a primitive form of an isotherm equation.

$$\ln\tilde{\rho}_1 + \frac{zr_1}{RT}\left[\tilde{\rho}_1\epsilon_{11} - \frac{\tilde{\rho}_1{}^2\epsilon_{11}}{2}\right] + r_1\left[\tilde{\rho}_1\left(1-\frac{1}{r_1}\right)\right] = \ln\theta_1 + \frac{zr_1}{RT}\left[\frac{-\theta_1{}^2\epsilon_{11}}{2} - \theta_1\theta_2\epsilon_{12} - \frac{\theta_2{}^2\epsilon_{22}}{2} + \theta_1\epsilon_{11} + \theta_2\epsilon_{12}\right] + r_1\left[\theta_1\left(1-\frac{1}{r_1}\right) + \theta_2\left(1-\frac{1}{r_2}\right)\right] \quad (16)$$

Introducing the assumption that $\theta_1 + \theta_2 \approx 1$ and the definition of the interaction parameter

$$\chi_{12} = \frac{z}{RT}\left(\epsilon_{12} - \frac{\epsilon_{11}+\epsilon_{22}}{2}\right) \quad (17)$$

the isotherm equation can be simplified to[28]

$$\ln\theta_1 + r_1\left(\frac{1}{r_2}-\frac{1}{r_1}\right)\theta_1 + r_1\chi_{12}(1-\theta_1)^2 = \ln\tilde{\rho}_1 + r_1\left(1-\frac{1}{r_1}\right)\tilde{\rho}_1 + r_1\left(\frac{-z\epsilon_{11}}{2RT}\right)(1-\tilde{\rho}_1)^2 + r_1\left(\frac{1}{r_2}-1\right) \quad (18)$$

Instead of obtaining the necessary values of T^* and ρ^* from pure component data, Martire and Boehm[28] used the critical properties $T_{c,1}$ and $\rho_{c,1}$ of CO_2 to obtain $\tilde{T}_1$ and $\tilde{\rho}_1$ from the relations

$$\frac{-z\epsilon_{11}}{RT} = \frac{1}{\tilde{T}_1} = \frac{(1+\sqrt{r_1})^2\,T_{c,1}}{r_1T}$$

and

$$\tilde{\rho}_1 = \frac{\rho_1}{\rho_{c,1}(1+\sqrt{r_1})}$$

As with the other treatments, an adjustable mixture parameter, ζ, was used to calculate χ_{12} from the relation

$$\chi_{12} = \frac{z}{RT}\left\{\zeta\sqrt{\epsilon_{11}\epsilon_{22}} - \frac{\epsilon_{11}+\epsilon_{22}}{2}\right\}$$

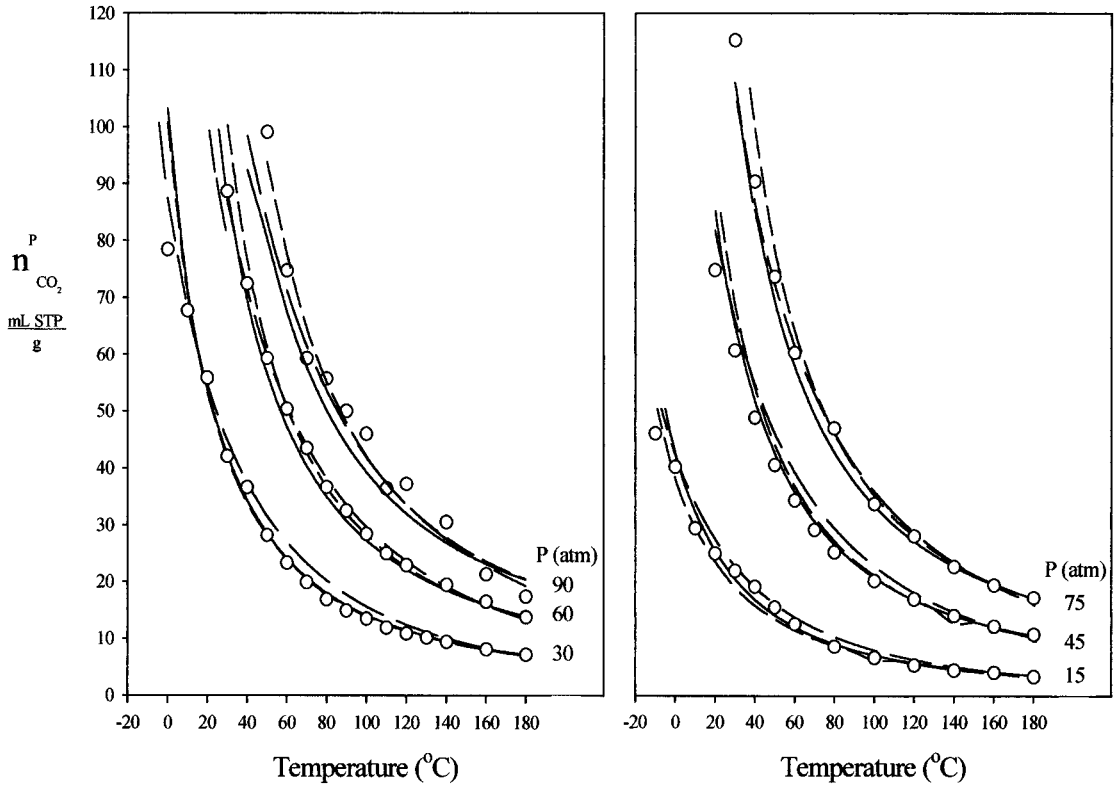

Figure 6. Theoretical and experimental solubility of CO_2 in PMMA: (—) Sanchez−Lacombe,[24−26] (- - -) Panayiotou−Vera,[12] (− −) Martire-Boehm,[28] (○) this study.

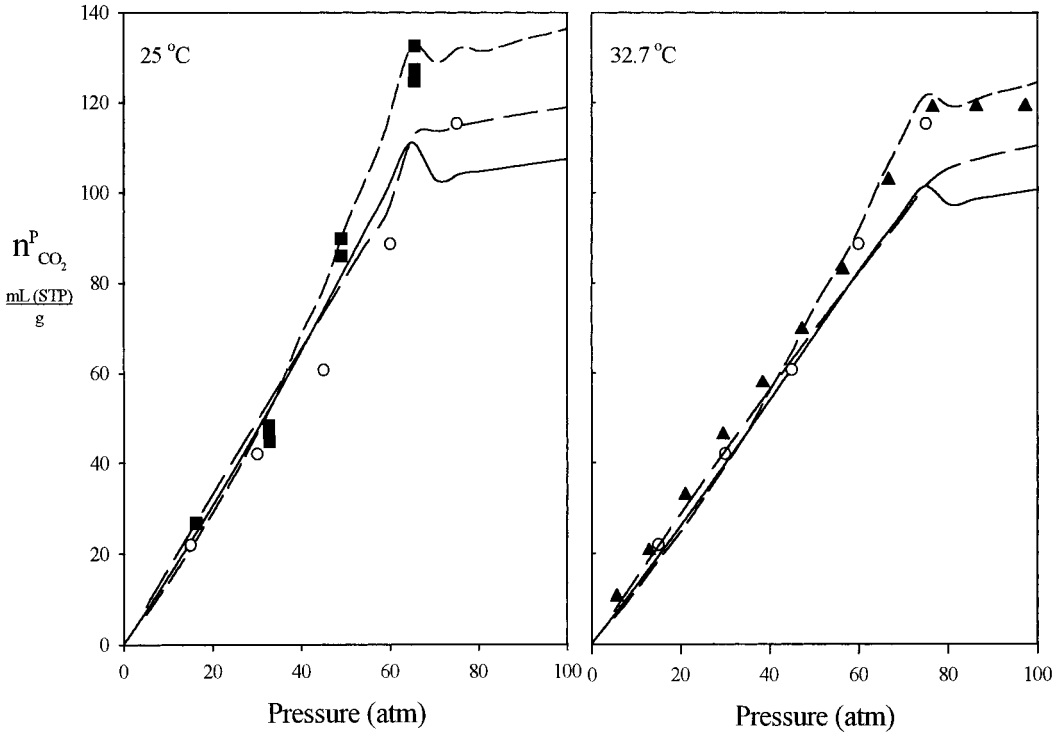

Figure 7. Sorption isotherms of CO_2 in PMMA: (—) Sanchez−Lacombe,[24−26] (- - -) Panayiotou−Vera,[12] (− −) Martire-Boehm,[28] (○) this study, (■) Berens and Huvard,[14] (▲) Wissinger and Paulaitis.[11]

The interaction energies were calculated from T^* values given by Condo et al.,[1] namely, $T_1^* = 308$ K and $T_2^* = 696$ K. The linear regression results for ζ were described by the equation $\zeta = 1.12 + 3.3 \times 10^{-4}t$ (°C) with a correlation coefficient of 0.89. The observed temperature dependence of ζ agreed fairly well for both the Martire−Boehm and Sanchez−Lacombe models.

Modeling Results. Figure 6 shows the experimental data from Table 1 along with the theoretical lines calculated from the three lattice fluid models examined in this investigation. The calculated theoretical lines agree within experimental error with the measured values. Each theoretical line was calculated with a single temperature-dependent adjustable parameter, ζ, involved in the calculation of either ϵ^* or P^*. The physical

meaning of the ζ is unclear because the P−V and S−L theories use the parameter differently. In the P−V model, ζ is a measure of the deviation of ϵ_{12} from the geometric mean of ϵ_{11} and ϵ_{22}. On the other hand, in the S−L treatment ζ is a measure of the deviation of P_{12} from the geometric mean of P_1* and P_2*. Thus, the two ζ parameters are not exactly equivalent. Nonetheless, under the conditions used in this study, each of the theoretical models accurately describes the solubility data within experimental error over the broad range of temperatures and pressures employed for the chromatographic experiments.

Figure 7 illustrates two isothermal data sets. Part A shows the 25 °C isotherm of Berens and Huvard,[14] whereas part B illustrates an isotherm at 32.7 °C published by Wissinger and Paulaitis.[11] Chromatographic data at 30 °C from this study are also presented with these literature isotherms. Calculated isotherms at these two temperatures were obtained using the three models discussed herein. At high pressures (above 50 atm) the three models vary in their prediction of CO_2 solubility in PMMA. The P−V theory seems to model the experimental data more accurately at these high pressures.

Conclusions

In a similar investigation, Garg et al.[29] found that the S−L EOS reproduced the density data for pure CO_2 better than the P−V EOS; however, the P−V model produced better fits to the measured solubility of CO_2 in poly(dimethylsiloxane) especially at higher pressures (P > 75 atm). This discrepancy was not observed in the present study mostly because the upper pressure was limited by the injection valve to 90 atm. Significantly, Garg et al. also found that ζ decreased with increasing temperature for 50, 80, and 100 °C.

While the three lattice models differ significantly, each model adequately describes the solubility of CO_2 in PMMA at least up to a pressure of 90 atm and over a 200 °C range of temperature. Notwithstanding their similar success in modeling the experimental data, the three lattice theories differ in their concepts and practical aspects. For example, the S−L model invokes the idea of a lattice that changes dimensions with composition, whereas the other two models avoid this concept by using a fixed value of v*. The P−V model allows for the nonrandom distribution of vacancies and r-mers on the lattice, which considerably complicates the mathematical calculations required. The M−B model employs the concept of Helmholtz free energy rather than the more commonly accepted Gibbs free energy. However, this considerably simplifies the numerical calculations, and the M−B approach also uses a fixed lattice site volume and random distribution of components and vacancies on the lattice sites. Accordingly, the M−B unified model is mathematically simpler than the other models but equal in accuracy at pressures < 90 atm.

Finally, the solubility data for CO_2 in PMMA obtained by tracer pulse chromatography are equivalent in accuracy and precision to that obtained with classical techniques. The available temperature and pressure ranges are extensive with common SFC instrumentation. Because of the thin film structure of the polymer phase and the forced flow imposed on the gas phase, equilibrium between the CO_2 in both the condensed and gas phases is achieved rapidly even with glassy polymers at low temperatures. In this study, for example, the equilibration time for experiments at 10 °C was less than 20 min at a pressure of 15 atm. Moreover, chromatographic methods can also be used to determine the glass transition temperatures of pure polymers and polymers impregnated with soluble gases such as CO_2 by measuring the retention volume (solubility) of a third component as a function of temperature.[30] For these many reasons, the application of chromatographic techniques to the measurement of the solubility of gases in polymers may lead to the establishment of a reliable database for the development and testing of solution theories for these complex, multicomponent systems.

Acknowledgment. This research was supported by a grant from the National Science Foundation. The authors also wish to express their appreciation to the Hewlett Packard Co. for the donation of the 5971 MSD system.

References and Notes

(1) Condo, P. D.; Sanchez, I. C.; Panayiotou, C. G.; Johnston, K. P. *Macromolecules* **1992**, *25*, 6119−6127.
(2) Parcher, J. F. *J. Chromatogr.* **1982**, *251*, 281−288.
(3) Hufton, J. R.; Danner, R. P. *AIChE J.* **1993**, *39*, 954−961.
(4) Parcher, J. F.; Bell, M. L.; Lin, P. J. *Advances in Chromatography*; Giddings, J. C., Ed.; Marcel Dekker: New York, 1984.
(5) Song, H.; Parcher, J. F. *Anal. Chem.* **1990**, *62*, 2616−2619.
(6) Koros, W. J.; Smith, G. N.; Stannett, V. *J. Appl. Polym. Sci.* **1981**, *26*, 159−170.
(7) Meares, P. *J. Am. Chem. Soc.* **1954**, *76*, 3415−3422.
(8) Sada, E.; Kumazawa, H.; Yakushiji, H.; Bamba, Y.; Sakata, K. *Ind. Eng. Chem. Res.* **1987**, *26*, 433−438.
(9) Kamiya, Y.; Mizoguchi, K.; Hirose, T.; Naito, Y. *J. Polym. Sci. Polym. Phys. Ed.* **1989**, *27*, 879−892.
(10) Liau, I. S.; McHugh, M. A. In *Supercritical Fluid Technology*; Penninger, J. M. L., Radosz, M., McHugh, M. A., Krukonis, V. J., Eds.; Elsevier: Amsterdam, 1985, pp 415−434.
(11) Wissinger, R. G.; Paulaitis, M. E. *J. Polym. Sci. Polym. Phys. Ed.* **1987**, *25*, 2497−2510.
(12) Panayiotou, C.; Vera J. H. *Polym. J.* **1982**, *14*, 681−694.
(13) Wissinger, R. G.; Paulaitis, M. E. *Ind. Eng. Chem. Res.* **1991**, *30*, 842−851.
(14) Berens, A. R.; Huvard, G. S. In *Supercritical Fluid Science and Technology*; Johnston, K. P., Penninger, J. M. L., Eds.; American Chemical Society: Washington, DC, 1989; pp 207−223.
(15) Panda, S.; Bu, Q.; Yun, K. S.; Parcher, J. F. *J. Chromatogr.* **1995**, *715*, 279−285.
(16) Prausnitz, J. M.; Lichtenthaler, R. N.; de Azevedo, E. G. *Molecular Thermodynamics of Fluid-Phase Equilibria*; Prentice-Hall: Englewood Cliffs, NJ, 1986; Chapter 7.
(17) Shim, J.-J.; Johnston, K. P. *AIChE J.* **1989**, *35*, 1097−1106.
(18) Peng, D. Y.; Robinson, D. B. *Ind. Eng. Chem. Fundam.* **1976**, *15*, 59−64.
(19) Fleming, G.; Koros, W. *Macromolecules* **1986**, *19*, 2285−2291.
(20) Olabisi, O.; Simha, R. *Macromolecules* **1975**, *8*, 206−210.
(21) Flory, P. J. *Principles of Polymer Chemistry*; Cornell University: Ithaca, NY, 1969.
(22) Etxeberria, A.; Iriarte, M.; Uriarte, C.; Iruin, J. J. *Macromolecules* **1995**, *28*, 7188−7195.
(23) Schuster, R. H.; Grater, H.; Cantow, H. J. *Macromolecules* **1984**, *17*, 619−625.
(24) Lacombe, R. H.; Sanchez, I. C. *J. Phys. Chem.* **1976**, *80*, 2568−2580.
(25) Sanchez, I. C.; Lacombe, R. H. *Macromolecules* **1978**, *11*, 1145−1156.
(26) Sanchez, I. C.; Lacombe, R. H. *J. Phys. Chem.* **1976**, *80*, 2352−2362.
(27) Wissinger, R. G. Ph.D. Dissertation, University of Delaware, 1988.
(28) Martire, D. E.; Boehm, R. E. *J. Phys. Chem.* **1987**, *91*, 2433−2446.
(29) Garg, A.; Gulari, E.; Manke, C. *Macromolecules* **1994**, *27*, 5643−5653.
(30) Parcher, J. F.; Edwards, R. R.; Yun, K. S. *Anal. Chem.* **1997**, *69*, 229A−234A.